Analytic computation of the strong stochasticity threshold in Hamiltonian dynamics using Riemannian geometry

Lapo Casetti
Dipartimento di Fisica, Università di Firenze, Largo Enrico Fermi 2, 50125 Firenze, Italy

Marco Pettini*
Osservatorio Astrofisico di Arcetri, Largo Enrico Fermi 5, 50125 Firenze, Italy
(Received 25 June 1993)

This paper concerns the study of the strong stochasticity threshold (SST) in Hamiltonian systems with many degrees of freedom, and more specifically the stability problem of this threshold in the thermodynamic limit ($N \to \infty$). The investigation is based on a recently proposed differential geometrical description of Hamiltonian chaos. The mathematical framework is given by Eisenhart's formulation of Newtonian mechanics in a suitably enlarged configuration space-time: a Riemannian manifold equipped with an affine metric. Using the Jacobi–Levi-Civita equation for geodesic spread, we estabilish a relation between curvature properties of the ambient manifold and the stability—or instability—of the dynamics. The use of the Eisenhart metric makes it clearly evident that a dominating source of chaoticity in Hamiltonian flows of physical interest is represented by *parametric resonance* induced by curvature fluctuations along the geodesics and not by negativeness of some curvature property. Here only Ricci curvature is involved because the scalar curvature vanishes *identically* with this metric. Thus a geometric quantity relevant to the study of chaos is the degree of bumpiness of the ambient manifold, i.e., the integral of the Ricci curvature carried over the whole manifold with the constraint of energy constancy. This quantity, considered as a function of the energy density ε, clearly marks the SST. A simple sufficient criterion is given to identify integrable systems and is here applied to a chain of linear oscillators as well as to the Toda lattice. In the case of the Fermi-Pasta-Ulam β model we have worked out *analytically* the ε dependence of the degree of bumpiness of the ambient manifold. This allowed us to prove that the SST is *stable* in the $N \to \infty$ limit. An operational definition of the critical energy density is also provided and shown to yield predictions in excellent agreement with previous results based on Lyapunov exponents.

PACS number(s): 05.45.+b, 02.40.−k, 05.20.−y

I. INTRODUCTION

It has been shown recently [1,2] that a strong stochasticity threshold (SST) exists in nonlinear Hamiltonian systems with $N \geq 3$ degrees of freedom. Generic nonintegrable Hamiltonian systems, with at least three degrees of freedom, always have a connected chaotic component in phase space. As already discussed elsewhere [1–3], the measure of such a chaotic fraction of phase space coincides with the measure of the whole accessible energy surface when the nonintegrable perturbation amplitude exceeds some critical value given by the Kol'mogorov-Arnol'd-Moser (KAM) theorem. But this critical value drops to zero faster than exponentially with the number of degrees of freedom. Already with a few tenths of degrees of freedom the KAM threshold is too small to have any physical relevance.

The SST is defined through a critical energy density ε_c ($\varepsilon = E/N$ is the energy per degree of freedom) such that for $\varepsilon > \varepsilon_c$ the dynamics is strongly chaotic, whereas for $\varepsilon < \varepsilon_c$ the dynamics is only weakly chaotic.

Strong chaoticity is quantitatively described by a scaling law of the largest Lyapunov exponent $\lambda_1(\varepsilon)$, explained by a random-matrix approximation of the tangent dynamics, and since at $\varepsilon > \varepsilon_c$ the tangent dynamics of the flow is reasonably approximated by a random-matrix process without memory, the dynamics itself must possess good properties of randomness (of course if it is observed with a suitable temporal coarse graining). In this case diffusion is fast in every direction of phase space and mixing is fast for the largest majority of initial conditions.

On the contrary, at $\varepsilon < \varepsilon_c$ phase-space diffusion is much slower and chaoticity is definitely weaker and characterized by a steeper scaling law $\lambda_1(\varepsilon)$. In this regime, depending on the initial conditions, very long mixing times can be observed. Phase-space paths are now more tortuous and can even look regular when followed during an insufficiently long observational time.

The discovery of this threshold (SST) has eventually clarified the reason why some kind of bimodality has always been found in the dynamical behavior of nonlinear, nonintegrable Hamiltonian systems. Such a bimodality, found in numerical simulations by varying the energy, has been attributed, from time to time, to the existence of a stochasticity threshold [4,5], the existence of an equipartition threshold [6], or tentatively explained through theoretical results such as the Nekhoroshev theorem [7]. However, the bimodality can be properly explained by a transition between regimes of a qualitatively different chaoticity, thus by the existence of the SST. In

fact, chaos is always present in nonlinear nonintegrable Hamiltonian systems, therefore we cannot properly speak of a stochasticity threshold.

Equipartition of energy is always attained [1,2] in the energy domains where insufficient observational times seem to suggest the contrary, so that an equipartition threshold cannot be properly defined (unless some bound is preassigned to observation time).

Finally, methods and results borrowed from classical perturbation theory are not adequate to account for the existence of the SST inasmuch as it concerns chaotic rather than regular motion and it occurs at a degree of nonlinearity far above the quasi-integrability condition.

A major question about this threshold has been left open: what is its fate when the number N of degrees of freedom becomes larger and larger? This is commonly referred to as the thermodynamic-limit problem. The present paper aims at giving a substantial contribution about this point.

Since a pioneering paper on a chain of particles coupled by a Lennard-Jones potential [8], some indications were found about a possible stability with N of the critical energy, at that time referred to as stochasticity threshold. Later on, results about an apparent existence of an equipartition threshold [6] seemed to confirm the above suggested stability whereas in a subsequent work [9] it has been claimed just the opposite.

There are at least three main points deserving particular care: (i) the definition of the threshold, (ii) the choice of initial conditions, and (iii) the choice of a sensible way of detecting the threshold.

A good definition of the SST could be given through the ε behavior of any observable that is sensitive to the difference between weak and strong chaos. A nice example is provided by quantities related to correlation functions [10]. However, the crossover of the scaling of $\lambda_1(\varepsilon)$ has some major advantages: it is unambiguous, directly related to the level of chaoticity, and is *independent of the choice of initial conditions.* Because of this last property, the crossover of $\lambda_1(\varepsilon)$ gives an *intrinsic* definition of a *global* transitional feature of the dynamics; for this reason it is markedly superior to any other observable.

A priori one could hope to get hints about the thermodynamic limit of the SST by working out $\varepsilon_c(N)$ from $\lambda_1(\varepsilon, N)$. Unfortunately the convergence time of $\lambda_1(t)$ quickly grows with N, becoming prohibitively long, at low energy, already at a few hundreds of degrees of freedom.

In order to circumvent this difficulty, we use, in the present paper, an alternative method to study both analytically and numerically the SST. This method is based on a differential geometrical description of Hamiltonian chaos [3].

The geometrical approach is made possible by Maupertuis's least-action principle for isoenergetic paths of standard (i.e., Newtonian) Hamiltonian systems. Kinetic energy provides a positive-definite quadratic form $a_{ik}\dot{q}^i\dot{q}^k$ allowing the definition of a Riemannian metric in configuration space M. The arc length, when a potential function is present, is $ds^2 = 2W^2dt^2 = \{[E - V(\mathbf{q})]a_{ik}\dot{q}^i\dot{q}^k\}dt^2 = g_{ik}dq^idq^k$.

The geodesic equations on a Riemannian manifold are given by

$$\frac{d^2q^\mu}{ds^2} + \Gamma^\mu_{\nu\rho}\frac{dq^\nu}{ds}\frac{dq^\rho}{ds} = 0 \ , \tag{1}$$

where s is the proper time and $\Gamma^\mu_{\nu\rho}$ are the Christoffel coefficients of the Levi-Civita connection associated with $g_{\mu\nu}$. By computing Eq. (1) with the kinetic-energy (Jacobi) metric, we recover Newton's equations of motion.

There is a relationship between the stability of the geodesics of a Riemannian manifold and the curvature properties of the same manifold. Such a relationship is based on a mathematical tool related with the second-order variations of the arc-length (action) functional. Equation (1) represents the differential version of the condition to make vanishing first-order variations of this functional. We can intuitively understand that a geodesic that makes stationary the arc-length (action) functional without minimizing it will be unstable with respect to variations of the initial conditions.

Second-order variations lead to Jacobi–Levi-Civita (JLC) equation of geodesic spread. This equation reads

$$\frac{\nabla}{ds}\frac{\nabla}{ds}\xi^\mu + R^\mu_{\nu\rho\sigma}\frac{dq^\nu}{ds}\xi^\rho\frac{dq^\sigma}{ds} = 0 \ , \tag{2}$$

where $\boldsymbol{\xi}$ is the vector field of geodesic separation and can be used to measure the distance between nearby geodesics; $(\nabla\boldsymbol{\xi}/ds)$ is the covariant derivative along a geodesic and $R^\mu_{\nu\rho\sigma}$ is the Riemann curvature tensor.

Now we can ask what the relationship between the instability of the geodesics and chaos is.

It is well known that a key for the understanding of deterministic chaos is provided by Smale's diffeomorphism: an abstract and paradigmatic way of realizing the two basic (topological) ingredients for the appearance of a hyperbolic limit set, i.e., *stretching* and *folding* of a given set of initial conditions [11].

The traditional explanation of the origin of chaos in Hamiltonian systems is provided by the existence of homoclinic intersections [12]. Especially at high dimension and for strong nonlinearity, homoclinic intersections are of little practical (computational) use; however, they are responsible for the appearance of a hyperbolic invariant set (Smale-Birkhoff theorem) deeply affecting the dynamics. Therefore Hamiltonian chaos also stems from the two mentioned basic ingredients—stretching and folding of volumes in phase space.

In the Riemannian description of Hamiltonian chaos, stretching is provided by the *instability* of nearby trajectories and folding by not allowing the distance between them to grow indefinitely, that is, by compactness of the ambient manifold. With these conditions, the phase trajectories are compelled to fold themselves in a very complicated fashion, which makes "forget" their initial conditions and makes their evolution practically unpredictable. This is an alternative way of looking at the origin of Hamiltonian chaos with respect to the standard approach of homoclinic intersections. For the majority of systems of physical interest, the configuration-space manifold (M, g_J) is compact, i.e., the coordinates remain

bounded during their time evolution.

For what concerns instability (stretching) of nearby geodesics, it can be studied by means of a scalar version of Eq. (2), obtained by standard algebraic manipulations, describing the evolution of the norm of the geodesic separation vector

$$\frac{1}{2}\frac{d^2\|\boldsymbol{\xi}\|^2}{ds^2}+\left(R_{\eta\nu\rho\sigma}\,\mu^\eta\frac{dq^\nu}{ds}\mu^\rho\frac{dq^\sigma}{ds}\right)\|\boldsymbol{\xi}\|^2-\left\|\frac{\nabla\boldsymbol{\xi}}{ds}\right\|^2=0\ , \tag{3}$$

where $\mu^\rho=\xi^\rho/\|\boldsymbol{\xi}\|$ are the components of the unit vector codirectional with $\boldsymbol{\xi}$. This equation is useful only if we can rewrite it in closed form. To this purpose some approximations must be introduced [3] and lead to

$$\frac{1}{2}\frac{d^2\|\boldsymbol{\xi}\|^2}{ds^2}+\tilde{\chi}\,\|\boldsymbol{\xi}\|^2-\left(\frac{d\|\boldsymbol{\xi}\|}{ds}\right)^2=0\ , \tag{4}$$

where $\tilde{\chi}$ is proportional to the Ricci curvature of the manifold.

In Sec. II we briefly recall some basic elements of the description of Hamiltonian dynamics in the enlarged configuration-space-time equipped with Eisenhart metric.

In Sec. III we define a criterion to compute the transition between weak and strong chaos. This criterion is applied to a chain of harmonic oscillators, as well as to the Toda lattice, to show how integrable models appear to be unambiguously characterizable. The same criterion, applied to the Fermi-Pasta-Ulam model, allows an analytic computation of the SST in the thermodynamic limit.

Some conclusions are drawn in Sec. IV.

II. EISENHART METRIC AND HAMILTONIAN DYNAMICS

As already pointed out in [3], there are several possible choices for the ambient manifold to rephrase Hamiltonian dynamics in geometrical terms: (i) configuration space M equipped with Jacobi metric g_J; (ii) configuration space-time $M\times\mathbb{R}$ with the structure of a Finsler space induced by a suitable metric g_F; (iii) enlarged configuration-space-time $M\times\mathbb{R}\times\mathbb{R}$ equipped with Eisenhart metric g_E; and (iv) tangent bundle TM of configuration space equipped with the Sasaki lift g_S of g_J and suitable restrictions to TM_E. Among the others, the Eisenhart metric has many advantages, as will become clear in the following.

The Riemannian structure of M is a consequence of Maupertuis least-action principle. In order to derive a Riemannian structure from Hamilton least-action principle, after the Eisenhart theorem [13] we must consider the enlarged configuration-space-time $M\times\mathbb{R}^2$ with local coordinates $q^0,q^1,\ldots,q^i,\ldots,q^N,q^{N+1}$, with $(q^1,\ldots,q^N)\in M$, $q^0\in\mathbb{R}$ is the time coordinate, and $q^{N+1}\in\mathbb{R}$ is given by [3]

$$q^{N+1}(t)=C_1^2t+C_2-\int_0^t L(\mathbf{q},\dot{\mathbf{q}})\,dt\ ; \tag{5}$$

C_1 and C_2 are arbitrary constants. For standard Hamiltonian functions $H=T+V(\mathbf{q})$, in this coordinate system the metric tensor g_E reads

$$g_E=\begin{pmatrix}-2V(\mathbf{q}) & 0 & \cdots & 0 & 1\\ 0 & a_{11} & \cdots & a_{1N} & 0\\ \vdots & \vdots & \ddots & \vdots & \vdots\\ 0 & a_{N1} & \cdots & a_{NN} & 0\\ 1 & 0 & \cdots & 0 & 0\end{pmatrix}\ , \tag{6}$$

hence the arc length of the manifold is given by

$$ds_E^2=a_{ij}dq^idq^j-2V(\mathbf{q})(dq^0)^2+2dq^0dq^{N+1}\ , \tag{7}$$

where a_{ij} is the kinetic-energy matrix. The inverse g_E^{-1} of the metric tensor, whose components are defined by

$$g^{\mu\nu}g_{\nu\sigma}=\delta^\mu_\sigma\ ,$$

takes the form

$$g_E^{-1}=\begin{pmatrix}0 & 0 & \cdots & 0 & 1\\ 0 & b_{11} & \cdots & b_{1N} & 0\\ \vdots & \vdots & \ddots & \vdots & \vdots\\ 0 & b_{N1} & \cdots & b_{NN} & 0\\ 1 & 0 & \cdots & 0 & 2V(\mathbf{q})\end{pmatrix}\ , \tag{8}$$

where $b_{ij}=(a_{ij})^{-1}$.

An nice property of this metric is that of giving an affine parametrization with time of the arc length; in fact one readily finds

$$ds_E^2=2C_1^2dt^2\ , \tag{9}$$

where C_1^2 is a real constant having the dimensions of an energy.

In the following, without loss of generality, we shall assume that the kinetic-energy matrix is diagonal, i.e., $a_{ij}=\delta_{ij}$. The only nonvanishing Christoffel coefficients are ($\partial_i=\partial/\partial q^i$, $i=1,\ldots,N$)

$$\Gamma^i_{00}=\partial_iV\ ,\qquad \Gamma^{N+1}_{0i}=-\partial_iV\ ; \tag{10}$$

hence the geodesic equations (1) become

$$\frac{d^2q^0}{ds^2}=0\ , \tag{11}$$

$$\frac{d^2q^i}{ds^2}+\Gamma^i_{00}\frac{dq^0}{ds}\frac{dq^0}{ds}=0\ , \tag{12}$$

$$\frac{d^2q^{N+1}}{ds^2}+\Gamma^{N+1}_{0i}\frac{dq^0}{ds}\frac{dq^i}{ds}=0\ , \tag{13}$$

and finally, using Eq. (9),

$$\frac{d^2q^0}{dt^2}=0\ , \tag{14}$$

$$\frac{d^2q^i}{dt^2}=-\frac{\partial V}{\partial q^i}\ , \tag{15}$$

$$\frac{d^2q^{N+1}}{dt^2}=-\frac{dL}{dt}\ . \tag{16}$$

Equation (14) states that $q^0=t$, the N equations (15) are just Newton equations of motion, and Eq. (16) is the differential version of the relation (5).

In Fig. 1, a pictorial representation is given of the enlarged configuration-space-time.

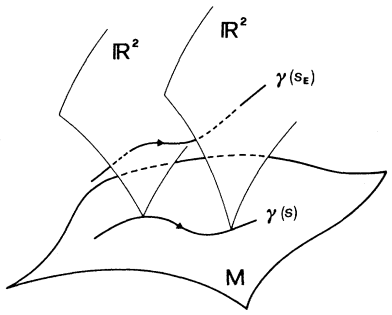

FIG. 1. Pictorial representation of the manifold $(M \times \mathbb{R}^2, g_E)$.

A. The Jacobi–Levi-Civita equation and the tangent dynamics

In comparison with Jacobi and Finsler metrics, the use of the Eisenhart metric has a great advantage: the simplicity in computing the relevant geometric quantities such as Riemann and Ricci tensors, etc. In particular, if the trajectories of a Hamiltonian system are seen as geodesics of the Eisenhart metric, then by studying their instability properties in the differential geometrical framework we recover a familiar tool in the analysis of the instability of the dynamics. In fact, the JLC equation (2) for the geodesic spread, for this metric, yields the usual *tangent dynamics equation* (26).

The equivalence between the geometric formulation of the instability problem and that in terms of the tangent dynamics is a consequence of the curvature properties of the manifold $(M \times \mathbb{R}^2, g_E)$. These are described by the Riemann tensor.

The nonvanishing components of the Riemann tensor are easily found to be

$$R_{0i0j} = \partial_i \partial_j V \ . \tag{17}$$

Hence we find that the Ricci tensor $R_{\mu\nu} = R^{\rho}_{\mu\rho\nu}$ has only one nonvanishing component

$$R_{00} = \partial^i \partial_i V = \triangle V \tag{18}$$

and that the scalar curvature $\mathcal{R} = R^{\mu}_{\mu}$ is everywhere vanishing:

$$\mathcal{R} \equiv 0 \ . \tag{19}$$

The JLC equation, written in components, then becomes [3]

$$\frac{\nabla}{ds}\frac{\nabla}{ds}\xi^0 + R^0_{i0j}\frac{dq^i}{ds}\xi^0\frac{dq^j}{ds} + R^0_{0ij}\frac{dq^0}{ds}\xi^i\frac{dq^j}{ds} = 0 \ , \tag{20}$$

$$\frac{\nabla}{ds}\frac{\nabla}{ds}\xi^i + R^i_{0j0}\left(\frac{dq^0}{ds}\right)^2\xi^j + R^i_{00j}\frac{dq^0}{ds}\xi^0\frac{dq^j}{ds} + R^i_{j00}\frac{dq^j}{ds}\xi^0\frac{dq^0}{ds} = 0 \ , \tag{21}$$

$$\frac{\nabla}{ds}\frac{\nabla}{ds}\xi^{N+1} + R^{N+1}_{i0j}\frac{dq^i}{ds}\xi^0\frac{dq^j}{ds} + R^{N+1}_{ij0}\frac{dq^i}{ds}\xi^j\frac{dq^0}{ds} = 0 \ . \tag{22}$$

Now we take advantage of (9) to replace ds with dt in both ordinary and covariant derivatives; then from (10) we know that $\Gamma^0_{ij} = 0$ so that

$$\frac{\nabla}{ds}\frac{\nabla}{ds}\xi^0 = \frac{d^2\xi^0}{dt^2} \ , \tag{23}$$

and, as $g^{00} = 0$ [Eq. (8)], all the mixed components of the Riemann tensor having a contravariant index equal to 0 vanish. Thus Eq. (20) becomes

$$\frac{d^2\xi^0}{dt^2} = 0 \ ; \tag{24}$$

by choosing separation vectors such that $\dot{\xi}^0(0) = \xi^0(0) = 0$, $\xi^0(t) = 0$, the components $1, \ldots, N$ of the covariant derivative also reduce to ordinary time derivatives and Eq. (21) reads

$$\frac{d^2\xi^i}{dt^2} + R^i_{0j0}\,\xi^j = 0 \ , \tag{25}$$

that is,

$$\frac{d^2\xi^i}{dt^2} + \frac{\partial^2 V}{\partial q_i \partial q^j}\xi^j = 0 \ , \tag{26}$$

which is the usual equation describing the tangent dynamics in the case of standard Hamiltonians.

We have here a very interesting result stemming from the use of the Eisenhart metric: the evolution equation for the vector field $\boldsymbol{\xi}$ of geodesic spread on the manifold $(M \times \mathbb{R}^2, g_E)$ reduces to the tangent dynamics equation in configuration space. The two additional equations are trivial; in fact, that concerning ξ^0 has the solution $\xi^0(t) = 0$, and Eq. (22) shows that ξ^{N+1} has only a passive evolution. In addition ξ^{N+1} does not influence the evolution of the other components and so it cannot contribute to any possible instability of the geodesics.

This result can be used to justify on different grounds the standard numerical algorithm [14] to compute Lyapunov exponents through a *local* averaging of the rate of exponential divergence of nearby trajectories. After having realized the geometrical origin of Eq. (26), the standard computational scheme turns out to be well defined on the basis of JLC equation with Eisenhart metric: there is no need for the Oseledeč theorem because numerical Lyapunov exponents are not *true* Lyapunov exponents [3].

B. Instability of the geodesics of $(M \times \mathbb{R}^2, g_E)$

The differential geometrical origin of Eq. (26) has another relevant consequence: it makes possible working out a *scalar* evolution equation for the norm of the separation vector obeying the equation for tangent dynamics. Such an equation is already given in [3] independently of the metric adopted, so it is straightforward to specialize it for the Eisenhart metric. It is worth noticing that such a derivation would be impossible starting just from the tangent dynamics equation. In fact, there is no natural criterion to derive from the vector equation (26) a scalar equation for the norm of $\boldsymbol{\xi}$.

The approximate evolution equation for the average norm ζ of the vector field $\boldsymbol{\xi}$ of geodesic separation reads [3]

$$\frac{d^2\zeta}{ds^2} + 2\chi(s)\zeta - \frac{1}{2\zeta}\left(\frac{d\zeta}{ds}\right)^2 = 0 \ , \tag{27}$$

where ζ is the norm of $\boldsymbol{\xi}$ after averaging over the possible directions of $\boldsymbol{\xi}$ at point P with an uniform distribution; $\chi(s)$ is the Ricci curvature per degree of freedom

$$\chi(s) = \frac{1}{N}K_R(s) = \frac{1}{N}R_{\mu\nu}\frac{dq^\mu}{ds}\frac{dq^\nu}{ds} \ . \tag{28}$$

In principle there is also another possibility of approximating the complete JLC equation. In fact, at any given point P, in addition to the average over the possible directions of $\boldsymbol{\xi}$, one could also average over the possible directions of the velocity vector of all the geodesics issuing from P. This would lead to $\chi(s) = \mathcal{R}/N^2$, where $\mathcal{R}$ is the scalar curvature at P. However, in the case of the Eisenhart metric it is found, Eq. (19), that $\mathcal{R} = 0$ *identically.*

By substituting in (28) the only nonvanishing component R_{00} of Ricci tensor in (18), we obtain

$$\frac{1}{N}K_R(s) = \frac{1}{N}\triangle V\left(\frac{dq^0}{ds}\right)^2 \ , \tag{29}$$

and since Eq. (9) means that dq^0/ds is a constant, Eq. (27) is now

$$\frac{d^2\zeta}{dt^2} + 2k_R(t)\zeta - \frac{1}{2\zeta}\left(\frac{d\zeta}{dt}\right)^2 = 0 \ , \tag{30}$$

where

$$k_R(t) = \frac{1}{N}\,\triangle V|_{\mathbf{q}(t)} \ . \tag{31}$$

The norm ζ is real and positive; thus we can put

$$\zeta(t) = \psi^2(t) \tag{32}$$

so that Eq. (30) is cast in the form of a generalized Hill equation

$$\frac{d^2\psi}{dt^2} + k_R(t)\,\psi = 0 \ . \tag{33}$$

The scalar equation (33) is perhaps the most concise non-trivial description of the stability properties of dynamical motions of a standard Hamiltonian flow.

As already discussed in the Introduction, chaos is the result of the combined presence of instability of the geodesics and compactness of the ambient manifold. Apparently some problem could arise in the case of $(M \times \mathbb{R}^2, g_E)$ because it is not compact. However, let us remember that natural motions are the projections on configuration space of the geodesics of $(M \times \mathbb{R}^2, g_E)$. In particular, the projections live in a compact subset of configuration space for most of the potentials of physical interest. Moreover, if the geodesics of $(M \times \mathbb{R}^2, g_E)$ are unstable, their projections will also be unstable, and thus natural motions in configuration space will be chaotic.

There are two possible ways of obtaining unstable solutions of Eq. (33), i.e., such that

$$\psi \sim e^{\lambda t} \qquad \Longrightarrow \qquad \zeta \sim e^{2\lambda t} \ ,$$

and hence chaos: $k_R(t)$ must be *negative* somewhere along a geodesic (loosely speaking, a positive measure of such regions of negative curvature is needed) or $k_R(t)$, being positive, must fluctuate in a suitable fashion in order to induce *parametric instability.*

There are potentials for which $k_R > 0$ always holds true [for instance, this is the case of the Fermi-Pasta-Ulam (FPU) model, lattice φ^4 model, etc.]. For others, such as the Lennard-Jones or the Morse potential, if the particle motions are essentially confined inside the binding region (where potential energy is smaller than dissociation energy) and below the inflection point of the potential, then we have again $k_R > 0$. This can be mainly the case of solid state systems.

When Ricci curvature is always positive, or it is positive for the overwhelming majority of points along a given trajectory, the only, or dominant, mechanism to make chaos is parametric resonance. The use of the Eisenhart metric provides a clear confirmation of the already emerged [3] relevance of this mechanism for Hamiltonian chaos.

As it is the bumpiness of the ambient manifold, rather than negative curvature, that is the dominant source of chaos, we will focus our attention on the global degree of bumpiness of $(M \times \mathbb{R}^2, g_E)$, i.e., on the mean Ricci curvature integrated over the whole manifold with the constraint of constant energy.

In Fig. 2 we report two numerical solutions of Hill's equation (33), for the FPU model, showing an exponential growth with time of the average norm of the separation vector. At higher energy instability is stronger. A systematic analysis of the ε dependence of the instability exponent obtained by solving Hill's equation (33) together with the dynamics will be given elsewhere.

III. A CRITERION TO COMPUTE THE TRANSITION FROM WEAK TO STRONG CHAOS

In the preceding section we have used simple elements of a geometric language to tackle Hamiltonian chaos in

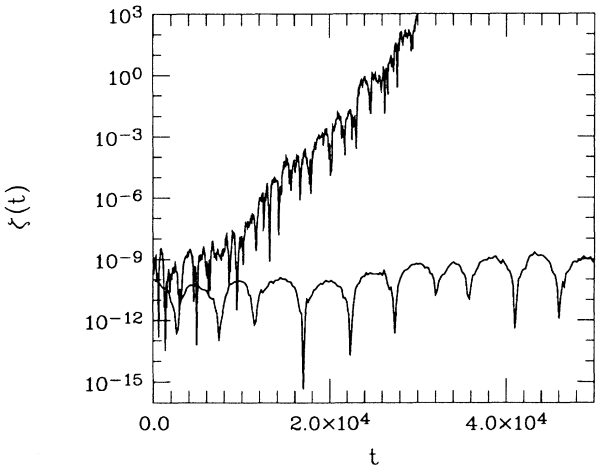

FIG. 2. Numerical solutions $\zeta(t) = \psi^2(t)$ of Hill's equation (33) for the FPU model at $N = 128$ and $\varepsilon = 0.6 < \varepsilon_c$ (bottom curve) and $\varepsilon = 6 > \varepsilon_c$ (top curve).

an alternative way, independently of homoclinic intersections. The geometric approach is definitely more natural because it makes use of natural coordinates instead of action-angle ones, it applies at any energy instead of being valid only in the quasi-integrable limit, and the deep origin of Hamiltonian chaos now becomes intuitively evident simply by studying the first and second variations of the action functional. The geometric approach has another nice property: it unifies the explanation of the origin of chaos and the way to measure its strength.

Now we want to show how powerful the geometric approach is by addressing a physically relevant problem already mentioned in the Introduction: the fate of the SST in the thermodynamic limit. A similar problem has been debated ever since the pioneering works that followed the FPU numerical experiment [15]. Before the present paper, no reliable argument has been put forward because of several reasons: only recently the SST has been discovered; beforehand a lot of confusion existed about what kind of transitional behavior is characteristic of many-dimensional Hamiltonian flows. The SST is in a privileged position because it is *independent of the choice of initial conditions*; thus it concerns a major global change of the structure of phase space that can be revealed by intrinsic properties of the dynamics with generic (random) initial conditions [1,2]. At variance, by adopting nonequilibrium initial conditions one gets only local information about the structure of phase space, and the complete arbitrariness in choosing such initial conditions makes it difficult to get a hold of any global transitional property. Moreover, until now the few attempts to find out the thermodynamic limit behavior of any transitional property of high-dimensional Hamiltonian flows were based on numerical scaling laws extrapolated at $N \to \infty$; such a procedure, being the only possible one with numerical simulations, is evidently rather dangerous.

In what follows, in order to work out *analytically* the specific energy (E/N) domains of weak and strong chaos, we adopt an effective criterion, already proposed in Ref. [3], which is here applied to the manifold $(M \times \mathbb{R}^2, g_E)$. The use of the Eisenhart metric now makes it easier to compute analytically the SST in the $N \to \infty$ limit.

The criterion is based on the observation that the average Ricci curvature of the ambient manifold, computed with the constraint of constant energy, is *independent* of energy density for integrable systems, both linear and nonlinear (i.e., a collection of harmonic oscillators and the Toda lattice). Hence the *ansatz* proposed in [3] follows: if the average Ricci curvature of the ambient manifold is constant with respect to energy density, then we are dealing with an integrable system; if the average Ricci curvature is *nearly* constant, that is, only weakly increasing with energy, then the system is in its weakly chaotic regime; finally, if the average Ricci curvature is *quickly* increasing with energy density, then the system is in its strongly chaotic regime. Since the transition is rather smooth, we conventionally define the energy threshold as the crossing value of the two asymptotes of the average Ricci curvature. This is a sensible criterion because it is in very good agreement with the crossover in the scaling of the largest Lyapunov exponent.

In other words, the bumpiness of the ambient manifold is responsible for the emergence of parametric instability, thus of chaos, and the rate of change with energy of the average bumpiness gives synthetic information about the degree of chaoticity of the dynamics. In Fig. 3 a pictorial representation is given of what is meant here.

A. Global geometric quantities

Let us now cope with the problem of computing the average value of any geometric quantity $f(\mathbf{q})$ on the whole manifold with the constraint $E = \text{const}$, i.e. on the constant-energy surface Σ_E with uniform measure. One has to compute

$$\langle f(\mathbf{q})\rangle_{\Sigma_E} = \frac{\int_{\Sigma_E} d\sigma_E\, f}{\int_{\Sigma_E} d\sigma_E} = \frac{1}{\Omega_E}\int f(\mathbf{q})\,\delta(H(\mathbf{q},\mathbf{p}) - E)d\mathbf{q}\,d\mathbf{p}\ , \qquad (34)$$

where

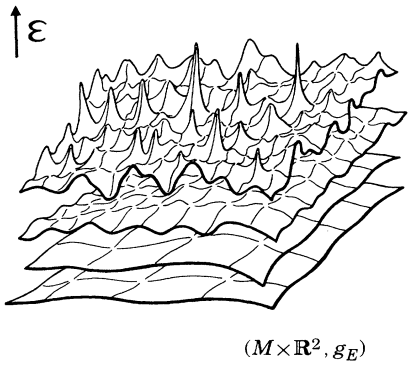

FIG. 3. Pictorial representation of the geometric change of the ambient manifold at increasing energy density ε.

$$\Omega_E = \int_{\Sigma_E} d\sigma_E = \int \delta(H(\mathbf{q},\mathbf{p}) - E) d\mathbf{q}\, d\mathbf{p} \ . \qquad (35)$$

Let us first compute Ω_E. By using

$$\delta(x) = \frac{1}{2\pi} \int_{-\infty}^{+\infty} e^{-i\alpha x} d\alpha$$

and setting $\eta = i\alpha$ we get

$$\Omega_E = \frac{1}{2\pi i} \int_{-\infty}^{+\infty} d\eta\, e^{\eta E} \int_{-\infty}^{+\infty} \prod_{i=1}^{N} dq_i dp_i\, e^{-\eta H(\mathbf{q},\mathbf{p})} \ .$$

Now, consider standard Hamiltonians

$$H(\mathbf{q},\mathbf{p}) = \frac{1}{2}\sum_{i=1}^{N} p_i^2 + V(\mathbf{q}) \ ; \qquad (36)$$

for these the integration over the p_i is trivial, and

$$\Omega_E = \frac{\pi^{N/2}}{2\pi i} \int_{-\infty}^{+\infty} d\eta\, \eta^{-N/2} e^{\eta E} \int_{-\infty}^{+\infty} \prod_{i=1}^{N} dq_i\, e^{-\eta V(\mathbf{q})} \ .$$

Here the multiple integral over the q_i is *formally* coincident with the configurational integral $Z_C(\eta)$ of statistical mechanics with the Gibbsian canonical measure, though in this case η is just a parameter and has nothing to do with temperature. So we can write

$$\begin{aligned} \Omega_E &= \frac{\pi^{N/2}}{2\pi i} \int_{-\infty}^{+\infty} d\eta\, \eta^{-N/2} e^{\eta E} Z_C(\eta) \\ &= \frac{\pi^{N/2}}{2\pi i} \int_{-\infty}^{+\infty} d\eta\, \exp\left[\eta E - \frac{N}{2}\ln\eta + \ln Z_C(\eta)\right] \ . \end{aligned}$$

This integral can be evaluated in the limit $N \to \infty$ by the saddle-point method; in fact, for $N \gg 1$, both E and $\ln Z_C$ are $O(N)$ quantities. Denoting with $\omega(\eta)$ the integrand, we have

$$\Omega_E = \omega(\overline{\eta}) \ ,$$

where $\overline{\eta}$ is the parameter value defined by the stationarity condition

$$\frac{\partial}{\partial\eta}\omega(\eta)\bigg|_{\eta=\overline{\eta}} = 0 \ ,$$

thus giving the relation between E and η

$$E - \frac{N}{2\eta} + \frac{\partial}{\partial\eta}\left[\ln Z_C(\eta)\right] = 0 \ .$$

In terms of the specific quantity $\varepsilon = E/N$, which is the relevant one in the limit $N \to \infty$, we have

$$\varepsilon(\eta) = \frac{1}{2\eta} - \frac{1}{N}\frac{\partial}{\partial\eta}\left[\ln Z_C(\eta)\right] \ . \qquad (37)$$

Finally we obtain $\Omega_E(\varepsilon)$ in *parametric* form as

$$\Omega_E(\epsilon) \begin{cases} \Omega_E(\eta) &= C_\eta Z_C(\eta) \\ \varepsilon(\eta) &= \dfrac{1}{2\eta} - \dfrac{1}{N}\dfrac{\partial}{\partial\eta}\left[\ln Z_C(\eta)\right], \end{cases} \qquad (38)$$

where C_η is inessential to compute the averages.

Let us now come to the computation of the average of $f(\mathbf{q})$. With the same reasoning just used for Ω_E, we can write

$$\langle f(\mathbf{q})\rangle_{\Sigma_E} = \frac{C_{\overline{\eta}} Z_C(\overline{\eta})}{\Omega_E(\overline{\eta})} \langle f\rangle^G(\overline{\eta}) = \langle f\rangle^G(\overline{\eta}) \ ,$$

where $\langle f\rangle^G$ is the Gibbsian average of f

$$\langle f\rangle^G = [Z_C(\eta)]^{-1} \int d\mathbf{q}\, f(\mathbf{q})\, e^{-\eta V(\mathbf{q})} \ . \qquad (39)$$

In conclusion, if one knows the canonical average (39) of f, one can also write the *parametric* equations for the average over Σ_E (34)

$$\langle f\rangle_{\Sigma_E}(\epsilon) \begin{cases} \langle f\rangle_{\Sigma_E}(\eta) &= \langle f\rangle^G(\eta) \\ \varepsilon(\eta) &= \dfrac{1}{2\eta} - \dfrac{1}{N}\dfrac{\partial}{\partial\eta}\left[\ln Z_C(\eta)\right] \ , \end{cases} \qquad (40)$$

which is *formally* also the microcanonical average of f.

B. Integrable systems

As already mentioned, in Ref. [3] it has been shown that the average Ricci curvature, computed for (M, g_J) with the constraint $(\mathbf{q},\mathbf{p}) \in \Sigma_E$, is independent of ε for two integrable systems: a chain of harmonic oscillators and the Toda lattice. This result has been obtained by Monte Carlo computations on Σ_E and by time averages along dynamical trajectories at $N = 128$ degrees of freedom.

Let us now check this result in the limit of arbitrarily large N and by using the Eisenhart metric. To this purpose remember that $k_R = \triangle V(\mathbf{q})/N$, so that

$$\langle k_R(\mathbf{q})\rangle_{\Sigma_E} = \frac{1}{\Omega_E}\int_{\Sigma_E} d\sigma_E \frac{1}{N}\triangle V(\mathbf{q}) \ . \qquad (41)$$

As linear integrable systems we consider a collection of N harmonic oscillators described by the Hamiltonians

$$H(\mathbf{p},\mathbf{q}) = \sum_{i=1}^{N} \frac{1}{2}p_i^2 + \frac{1}{2}(q_{i+1} - q_i)^2 \ , \qquad (42a)$$

$$H(\mathbf{p},\mathbf{q}) = \sum_{i=1}^{N} \frac{1}{2}p_i^2 + \frac{1}{2}\omega_i^2 q_i^2 \ . \qquad (42b)$$

We immediately find $k_R(\varepsilon) = 2$ and $k_R(\varepsilon) = \sum_{i=1}^{N}\omega_i^2/N$, respectively; hence

$$\langle k_R\rangle_{\Sigma_E}(\varepsilon) = 2 \ , \qquad (43a)$$

$$\langle k_R\rangle_{\Sigma_E}(\varepsilon) = \sum_{i=1}^{N}\frac{\omega_i^2}{N} = \text{const.} \qquad (43b)$$

If the frequencies ω_i in (42b) are given by $\omega_i = 2\sin(\pi i/N)$, then the q_i are the normal mode coordinates that diagonalize the Hamiltonian (42a). In this case the constant in Eq. (43b) is again 2.

Notice that in the generalized Hill equation (33) we have $k_R(t) = \text{const}$ for both systems; thus only periodic bounded oscillations of the norm of geodesic separation vector are possible, and this is true for *any* initial condition and at *any* energy.

As a nonlinear integrable system we consider the Toda lattice described by a standard Hamiltonian (36) with the potential function given by

$$V(\mathbf{q}) = \sum_{i=1}^{N}[e^{-(q_{i+1}-q_i)} + (q_{i+1} - q_i) - 1] \; ; \tag{44}$$

in this case the Ricci curvature reads

$$k_R = \frac{2}{N}\sum_{i=1}^{N} e^{-(q_{i+1}-q_i)} \; , \tag{45}$$

and as shown in Appendix A we get

$$\langle k_R \rangle_{\Sigma_E}(\varepsilon) = 2 \tag{46}$$

also for the Toda lattice. Here $k_R(t)$ entering Eq. (33) is no longer a constant along a trajectory. Nevertheless, things self-adjust so as to avoid parametric instability, as is shown in Fig. 4.

In conclusion, a sufficient mark of integrability, and so of regular dynamics, appears to be $\langle k_R \rangle_{\Sigma_E}(\varepsilon) = \text{const}$.

C. Computation of the SST in the FPU β model

Let us now consider a nonlinear nonintegrable system: the FPU β model described by the Hamiltonian

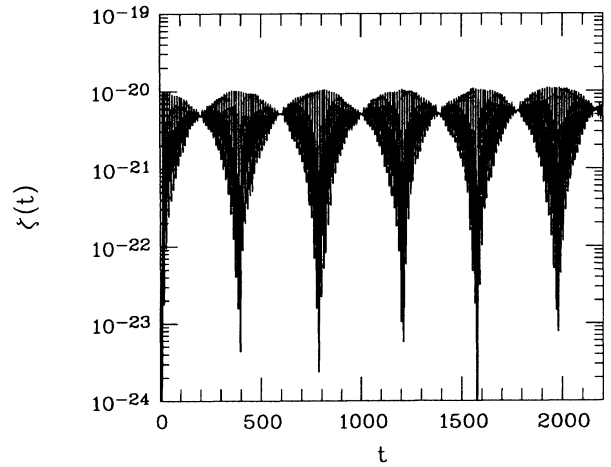

FIG. 4. Numerical solution $\zeta(t) = \psi^2(t)$ of Hill's equation (33) for the Toda lattice at $N = 128$ and $\varepsilon = 0.5$.

$$H = \sum_{i=1}^{N}\frac{1}{2}p_i^2 + \sum_{i=1}^{N}\left[\frac{1}{2}(q_{i+1} - q_i)^2 + \frac{\mu}{4}(q_{i+1} - q_i)^4\right] \; . \tag{47}$$

For this model, the geometric approach, based on the Eisenhart metric, makes possible the analytic study of the SST in the thermodynamic limit. The results so obtained are in excellent agreement with those reported in [3] at finite N and for (M, g_J). In particular, the study of the curvature properties of $(M \times \mathbb{R}^2, g_E)$ clearly shows the persistence of the transition between weak and strong chaos in the limit $N \to \infty$.

Again we have to compute the average Ricci curvature as a function of ε. To this purpose we use Eqs. (40) and (41). The explicit expression of the mean Ricci curvature k_R for the FPU β model (47) is

$$k_R = 2 + \frac{6\mu}{N}\sum_{i=1}^{N}(q_{i+1} - q_i)^2 \; . \tag{48}$$

Notice that for this model k_R is *always positive*, so that *parametric instability* is the only mechanism to make chaos, at least when the problem is treated with the aid of the Eisenhart metric and of the approximate equation (27).

In order to compute the Gibbsian average of k_R , which is needed to apply Eq. (40), we slightly modify the canonical partition function Z_C as follows:

$$\tilde{Z}_C(\alpha) = \int_{-\infty}^{+\infty}\prod_{i=1}^{N} dq_i \exp[-\eta\tilde{V}(\mathbf{q})] \; , \tag{49}$$

with

$$\tilde{V}(\mathbf{q}) = \sum_{i=1}^{N}\left[\frac{\alpha}{2}(q_{i+1} - q_i)^2 + \frac{\mu}{4}(q_{i+1} - q_i)^4\right] \; .$$

Equation (49) can be expressed in terms of Z_C and of the arbitrary parameter α as $\tilde{Z}_C(\alpha) = Z_C(\alpha\eta, \mu/\alpha)$, and hence we can write

$$\langle k_R \rangle(\eta) = 2 - \frac{12\mu}{\eta N}\frac{1}{Z_C}\left[\frac{\partial}{\partial\alpha}\tilde{Z}_C(\alpha)\right]_{\alpha=1} \; . \tag{50}$$

The problem of computing $\langle k_R \rangle$ is now reduced to that of working out

$$\frac{1}{NZ_C}\left[\frac{\partial}{\partial\alpha}\tilde{Z}_C(\alpha)\right]_{\alpha=1} = \frac{1}{N}\left[\frac{\partial}{\partial\alpha}\ln\tilde{Z}_C(\alpha)\right]_{\alpha=1} \; . \tag{51}$$

From the expression (49) for the partition function of the FPU β model, we can write

$$\tilde{Z}_C(\alpha) = [\tilde{z}_C(\alpha)]^N f(\alpha) \; , \tag{52}$$

where $f(\alpha)$ is a quantity $\sim O(1)$ and $\tilde{z}_C(\alpha)$ is the single-particle partition function [16]

$$\tilde{z}_C(\alpha) = \Gamma\left(\frac{1}{2}\right)\left(\frac{\eta\mu}{2}\right)^{-1/4}\exp\left(\frac{1}{4}\alpha^2\theta^2\right)D_{-1/2}(\alpha\theta) \; , \tag{53}$$

Γ is the Euler's function, $D_{-1/2}$ is a parabolic cylinder function, and

$$\theta = \left(\frac{\eta}{2\mu}\right)^{1/2} . \tag{54}$$

Therefore we can write

$$\frac{1}{N}\frac{\partial}{\partial\alpha}\ln\tilde{Z}_C(\alpha) = \frac{\partial}{\partial\alpha}\ln\tilde{z}_C(\alpha) + O\left(\frac{1}{N}\right) .$$

Thus in the thermodynamic limit Eq. (51) becomes

$$\frac{1}{N}\left[\frac{\partial}{\partial\alpha}\ln\tilde{Z}_C(\alpha)\right]_{\alpha=1} = \left[\frac{\partial}{\partial\alpha}\ln\tilde{z}_C(\alpha)\right]_{\alpha=1} . \tag{55}$$

By using standard properties of the parabolic cylinder functions, Eq. (55) reads

$$\left[\frac{\partial}{\partial\alpha}\ln\tilde{z}_C(\alpha)\right]_{\alpha=1} = -\frac{\theta}{2}\frac{D_{-3/2}(\theta)}{D_{-1/2}(\theta)} , \tag{56}$$

and going back to Eq. (50) through (56), (55), and (51) $\langle k_R\rangle$ is found as a function of the parameter θ

$$\langle k_R\rangle(\theta) = 2 + \frac{3}{\theta}\frac{D_{-3/2}(\theta)}{D_{-1/2}(\theta)} . \tag{57}$$

According to the (40), $\langle k_R\rangle$, averaged on Σ_E, is given in parametric form by (57) together with the implicit expression (37): $\varepsilon = \varepsilon(\eta)$.

Having in mind Eqs. (53) and (52), we find

$$-\frac{1}{N}\frac{\partial}{\partial\eta}\ln Z_C = \frac{1}{8\mu}\left[\frac{1}{\theta^2} + \frac{1}{\theta}\frac{D_{-3/2}(\theta)}{D_{-1/2}(\theta)}\right] ,$$

and the final expression relating θ and ε is

$$\varepsilon(\theta) = \frac{1}{8\mu}\left[\frac{3}{\theta^2} + \frac{1}{\theta}\frac{D_{-3/2}(\theta)}{D_{-1/2}(\theta)}\right] . \tag{58}$$

Finally, the average Ricci curvature of $(M\times\mathbb{R}^2, g_E)$, computed on Σ_E, is

$$\langle k_R\rangle(\varepsilon)\begin{cases} \langle k_R\rangle(\theta) &= 2 + \dfrac{3}{\theta}\dfrac{D_{-3/2}(\theta)}{D_{-1/2}(\theta)} \\ \\ \epsilon(\theta) &= \dfrac{1}{8\mu}\left[\dfrac{3}{\theta^2} + \dfrac{1}{\theta}\dfrac{D_{-3/2}(\theta)}{D_{-1/2}(\theta)}\right] . \end{cases} \tag{59}$$

In Fig. 5(b) $\langle k_R\rangle(\varepsilon)$ is plotted for the case $\mu = 0.1$, which has been chosen to make the comparison easier with previous results on the SST, obtained by numerical simulations [1,2]; in Fig. 5(a) the values of $\lambda_1(\varepsilon)$ which clearly show the crossover defining the SST are reported. Time averages $\overline{k_R}$

$$\overline{k_R} = \frac{1}{\tau}\int_0^\tau k_R[\mathbf{q}(t)]\,dt$$

have also been computed along numerical trajectories obtained at different values of ε and for $N = 128, 512$. The comparison among analytic and numeric results is made in Fig. 5(b). The agreement is strikingly good. It is worth noticing that already at $N = 128$, at least as far as these geometric properties are concerned, we have a very good indication about some asymptotic properties of the system.

These results indirectly confirm the correctness of similar ones already found in Ref. [3] by means of numerical simulations performed using Jacobi metric. The neat change of the ε dependence of $\langle k_R\rangle$ is well evident in Figs. 5(b) and 6. Moreover, the analytic result allows affirming safely that this effect is persistent in the thermodynamic limit $N \to \infty$.

The interpretation of the transition between weak and strong chaos (SST) (an effect due to the change of global

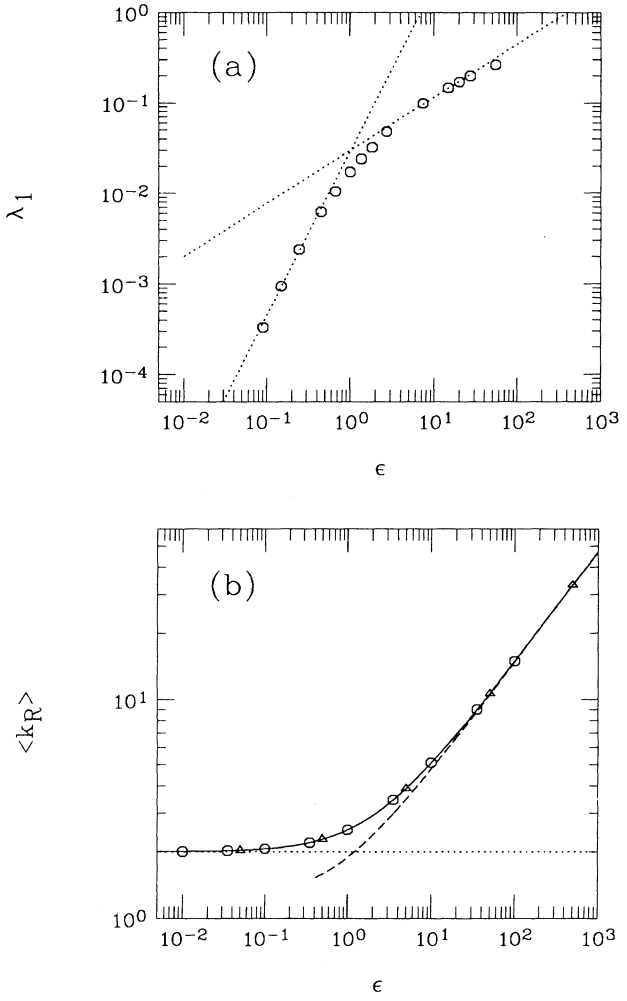

FIG. 5. Evidence of the SST in the FPU β model. (a) Largest Lyapunov exponent λ_1 (circles) computed by means of numerical simulation of the tangent dynamics with $N = 128$ and $\mu = 0.1$ (from Refs. [1,2]); dotted lines are references to power laws ε^2 and $\varepsilon^{2/3}$, and their intersection defines the SST. (b) Average Ricci curvature per degree of freedom $\langle k_R\rangle_{\Sigma_E}$ computed with $\mu = 0.1$. The continuous curve is the analytic result $\langle k_R\rangle_{\Sigma_E}(\varepsilon)$ (59); open circles and triangles are time averages $\overline{k_R}$ obtained by numerical simulation of the dynamics with $N = 128$ (circles) and $N = 512$ (triangles). Dotted and dashed lines are the asymptotic behaviors which are used to define the SST (see text and Fig. 7).

geometric properties of the Riemann manifolds underlying the trajectories of the system) is strengthened here.

Computation of the critical energy density of the SST

From the result of Eq. (59) one can derive an *analytic* expression for the critical energy density ε_c of the SST. This transition is *smooth*, i.e., neither the function $\langle k_R\rangle(\varepsilon)$ nor its derivatives has any discontinuity. Nevertheless, $\langle k_R\rangle(\varepsilon)$ shows two very different asymptotic behaviors at $\varepsilon \to 0$ and $\varepsilon \to \infty$; the first limit corresponds to the harmonic limit of the system

$$\varepsilon \to 0 \quad \Longrightarrow \quad \langle k_R\rangle(\varepsilon) \to \langle k_R\rangle_0 = 2 \ . \tag{60}$$

The tabulation of $\langle k_R\rangle(\varepsilon)$ shows that its high-energy behavior scales as $\varepsilon^{1/2}$, but we can find an analytic approximation for this limit. As $\varepsilon \to \infty \Rightarrow \theta \to 0$, one can expand the functions D_ν in Eq. (59) up to the first order in θ near $\theta = 0$, getting $D_{-1/2}(\theta) \sim D_{-1/2}(0) + D'_{-1/2}(0)\theta = D_{-1/2}(0) - \frac{1}{2}D_{-3/2}(0)\theta$ and $D_{-3/2}(\theta) \sim D_{-3/2}(0) + D'_{-3/2}(0)\theta = D_{-3/2}(0) - D_{-1/2}(0)\theta$. Then retaining again only the first-order terms in θ

$$\frac{D_{-3/2}(\theta)}{D_{-1/2}(\theta)} \sim \frac{D_{-3/2}(0) - D_{-1/2}(0)\theta}{D_{-1/2}(0) - \frac{1}{2}D_{-3/2}(0)\theta} \sim \frac{D_{-3/2}(0)}{D_{-1/2}(0)} + \frac{D^2_{-3/2}(0) - 2D^2_{-1/2}(0)}{2D^2_{-1/2}(0)}\theta \ .$$

Let us denote by $\langle k_R\rangle(\varepsilon) \to \langle k_R\rangle_\infty(\varepsilon)$ the asymptotic behavior in the limit $\varepsilon \to \infty$.

The parametric expression for $\langle k_R\rangle_\infty(\varepsilon)$ is

$$\langle k_R\rangle_\infty(\varepsilon) \begin{cases} \langle k_R\rangle_\infty(\theta) = 2 + \dfrac{D^2_{-3/2}(0) - 2D^2_{-1/2}(0)}{2D^2_{-1/2}(0)} + \dfrac{3}{\theta}\dfrac{D_{-3/2}(0)}{D_{-1/2}(0)} \\ \varepsilon_\infty(\theta) = \dfrac{1}{8\mu}\left[\dfrac{3}{\theta^2} + \dfrac{1}{\theta}\dfrac{D_{-3/2}(0)}{D_{-1/2}(0)} + \dfrac{D^2_{-3/2}(0) - 2D^2_{-1/2}(0)}{2D^2_{-1/2}(0)}\right] . \end{cases} \tag{61}$$

In Fig. 7 the two asymptotic behaviors are shown. The intersection point between the two asymptotes can be used as an *operational* definition of the threshold energy ε_c.

Let us now *define* ε_c through the condition

$$\langle k_R\rangle_0 = \langle k_R\rangle_\infty(\varepsilon_c) \ ,$$

and, by eliminating θ, from (61) we get the formula

$$\varepsilon_c = \frac{3}{32\mu}\frac{[D^2_{-3/2}(0) - 2D^2_{-1/2}(0)]^2}{D^2_{-1/2}(0)D^2_{-3/2}(0)} \ . \tag{62}$$

Substituting the numerical values [17]

$$\varepsilon_c \simeq \frac{0.121}{\mu} \ . \tag{63}$$

For $\mu = 0.1$ it is $\varepsilon_c \simeq 1.21$, which is in very good agreement with the recent numerical values determined through the crossover in the scaling behavior $\lambda_1(\varepsilon)$ of the largest Lyapunov exponent [1,2] or by geometric methods with Jacobi metric in [3].

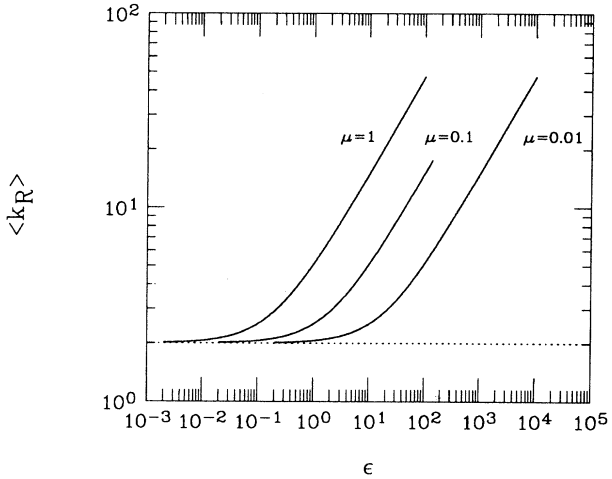

FIG. 6. Behavior of the Ricci curvature (59) for the FPU β model with different values of the nonlinear coupling constant μ.

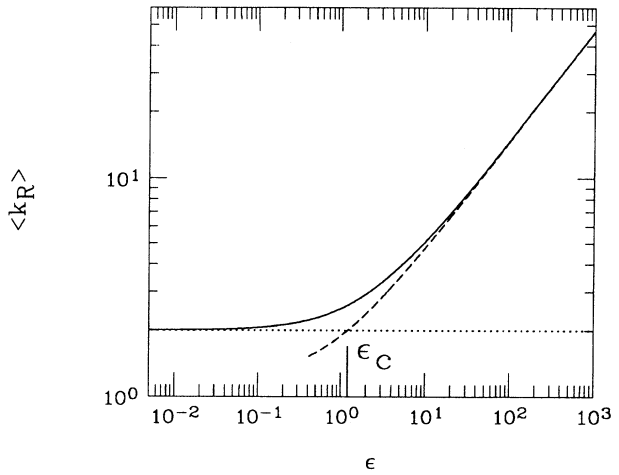

FIG. 7. Asymptotic behaviors of $\langle k_R\rangle_{\Sigma_E}$ for the FPU β model with $\mu = 0.1$. The continuous curve is the full result (59), the dotted line is the harmonic limit (60), and the dashed line is the high-energy limit (61). The intersection of these two curves defines ε_c.

Equation (62) gives ε_c as a function of the nonlinear coupling constant μ, and so we get a "critical line," in the parameter plane (ε, μ) of the FPU β model, separating the regions of weak and strong chaos; this is shown in Fig. 8.

IV. CONCLUSIONS

The present paper is a followup of a previous one where it has been shown that a Riemannian approach to the quantitative description of Hamiltonian chaos is powerful from both the conceptual and computational point of view. Here we have mainly investigated the potentialities of the Eisenhart metric on the enlarged configuration-space-time $(M \times \mathbb{R}^2, g_E)$.

Here we have found a confirmation of the fact that weak and strong chaoticity regimes, as well as the transition between them, are clearly marked by the energy dependence of a global geometric quantity—the mean Ricci curvature averaged over the whole manifold with the constraint of constant energy—moreover that the energy independence of the same quantity constitutes a sufficient and clear-cut method of recognizing integrable systems [3].

While confirming the power and the interest of the differential-geometrical description of Hamiltonian chaos, the present paper provides relevant results that can be summarized as follows: (i) the dominant source of chaos, in those systems whose particles interact through a confining potential, is *parametric resonance* due to fluctuations of positive Ricci curvature; (ii) the energy dependence of the mentioned geometric quantity can be computed with the same degree of difficulty of standard statistical-mechanical calculations and for both the FPU β model and the Toda lattice (in one dimension) we have worked out *exact analytic* computations in the $N \to \infty$ limit; (iii) we have given a proof of the stability of the strong stochasticity threshold in the thermodynamic limit; and (iv) we have provided a criterion to compute the transition energy ε_c of the SST. This criterion can be applied to the FPU model leading to an analytic formula for ε_c in the thermodynamic limit, the numeric value thus obtained is in excellent agreement with its previous determination through the crossover in the ε scaling of the largest Lyapunov exponent.

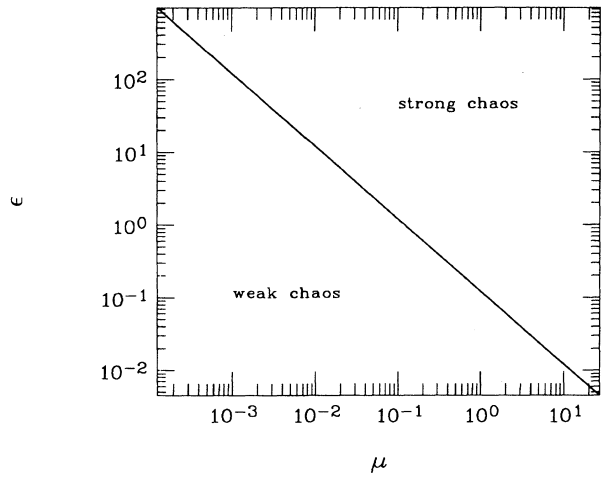

FIG. 8. Parameter plane (ε, μ) for the FPU β model with the "critical line" for the SST defined by Eq. (62).

ACKNOWLEDGMENT

It is a pleasure to thank R. Livi for friendly discussions.

APPENDIX A: COMPUTATION OF $\langle k_R \rangle_{\Sigma_E}$ FOR THE TODA LATTICE

The computation of $\langle k_R \rangle_{\Sigma_E}$ with the potential function of the one-dimensional Toda lattice (44) can be carried on, as already done for the FPU model. The Ricci curvature per degree of freedom is given by [Eq. (45)]

$$k_R = \frac{2}{N} \sum_{i=1}^{N} e^{-(q_{i+1}-q_i)} ,$$

and with the saddle-point method, as in Eq. (40), its average is

$$\langle k_R \rangle_{\Sigma_E}(\varepsilon) \begin{cases} \langle k_R \rangle(\eta) = -\dfrac{2}{N\eta} \dfrac{\partial}{\partial \alpha} [\ln \tilde{Z}_C(\alpha)]_{\alpha=1} \\ \varepsilon = \varepsilon(\eta) , \end{cases} \tag{A1}$$

where

$$\tilde{Z}_C(\alpha) = \int_{-\infty}^{+\infty} \prod_{i=1}^{N} dq_i \exp[-\eta \tilde{V}(\mathbf{q})] \tag{A2}$$

and

$$\tilde{V}(\mathbf{q}) = \sum_{i=1}^{N} \left[\alpha e^{-(q_{i+1}-q_i)} + (q_{i+1} - q_i) - 1 \right] . \tag{A3}$$

Moreover, for $N \to \infty$

$$\tilde{Z}_C(\alpha) \to [\tilde{z}_C(\alpha)]^N \tag{A4}$$

with

$$\begin{aligned} \tilde{z}_C(\alpha) &= \int_{-\infty}^{+\infty} dx \, \exp\left(-\eta \alpha e^{-x} - \eta x + 1\right) \\ &= \Gamma(\eta)(\eta\alpha)^{-\eta} e^{\eta} , \end{aligned} \tag{A5}$$

and by substituting Eqs. (A4) and (A5) into the first equation of (A1) we finally obtain

$$\langle k_R \rangle(\eta) = -\frac{2}{\eta} \frac{\partial}{\partial \alpha} \ln \tilde{z}_C(\alpha) \Big|_{\alpha=1} = -\frac{2}{\eta} \left[-\frac{\eta}{\alpha} \right]_{\alpha=1} = 2 \tag{A6}$$

and thus

$$\langle k_R \rangle_{\Sigma_E}(\varepsilon) = \langle k_R \rangle(\eta) = 2 . \tag{A7}$$

APPENDIX B: NUMERICAL COMPUTATIONS

A very efficient and precise symplectic algorithm has been proposed recently [18]. This integrator alternates two different choices of the function generating the canonical transformation that maps coordinates and momenta from any time t to a subsequent time $t + \Delta t$. For this reason the algorithm is called "bilateral."

Let us recall that the well-known leap-frog scheme which, for Hamiltonians such as $H(\mathbf{q},\mathbf{p}) = \sum_{i=1}^{N} p_i^2/2 + V(\mathbf{q})$, reads

$$\begin{aligned} q_i(t+\Delta t) &= q_i(t) + \Delta t\, p_i(t) \ , \\ p_i(t+\Delta t) &= p_i(t) - \Delta t \frac{\partial}{\partial q_i} V(\mathbf{q}(t+\Delta t)) \ , \end{aligned} \tag{B1}$$

is a canonical transformation of variables generated by the function

$$F(\mathbf{Q},\mathbf{p},\Delta t) = -\mathbf{Q}\cdot\mathbf{p} + \Delta t H(\mathbf{Q},\mathbf{p}) \tag{B2}$$

(lowercase letters $\mathbf{p}$ and $\mathbf{q}$ refer to time t, while capital letters refer to the same variables at time $t + \Delta t$).

At infinitesimal Δt, the function (B2) becomes exactly the generating function of the natural motion of the system in phase space [19]. There is some arbitrariness in the choice of (B2) to construct the numerical integration scheme. In fact, a function Φ obtained from (B2) by interchanging the role played by the coordinates with that of their conjugated momenta,

$$\Phi(\mathbf{q},\mathbf{P},\Delta t) = \mathbf{q}\cdot\mathbf{P} + \Delta t H(\mathbf{q},\mathbf{P}) \, , \tag{B3}$$

has the same meaning of F for a vanishing Δt; the transformation generated by (B3) is in fact an alternative form for the leap-frog algorithm.

The difference between these two limits shows up only at finite Δt, and so it has practical consequences only when these canonical transformations are used in the form of numerical integration algorithms. Hence the simple idea of compensating the errors of each partial scheme by alternating them in a bilateral algorithm results [18].

Moreover, by applying this idea to the general scheme to generate higher-order symplectic algorithms reported in Ref. [20], a second-order bilateral algorithm is worked out [18] in the following form:

$$\begin{aligned} \tilde{q}_i &= q_i(t) \ , \\ \tilde{p}_i &= p_i(t) - \frac{1}{2}\Delta t \frac{\partial}{\partial \tilde{q}_i} V(\tilde{\mathbf{q}}) \ , \\ q_i(t+\Delta t) &= \tilde{q}_i + \Delta t\, \tilde{p}_i \ , \\ p_i(t+\Delta t) &= \tilde{p}_i - \frac{1}{2}\Delta t \frac{\partial}{\partial q_i} V(\mathbf{q}(t+\Delta t)) \ , \\ \hat{p}_i &= p_i(t+\Delta t) \ , \\ \hat{q}_i &= q_i(t+\Delta t) + \frac{1}{2}\Delta t\, \hat{p}_i \ , \\ p_i(t+2\Delta t) &= \hat{p}_i - \Delta t \frac{\partial}{\partial \hat{q}_i} V(\hat{\mathbf{q}}) \ , \\ q_i(t+2\Delta t) &= \hat{q}_i + \frac{1}{2}\Delta t\, p_i(t+2\Delta t) \, . \end{aligned} \tag{B4}$$

The numerical integrations of both the FPU and the Toda lattice models have been performed with $\Delta t = 0.01$ at low and intermediate energy; at high energy Δt is scaled with energy so as to keep the energy fluctuations at the same order of magnitude. With this choice of Δt and with (B4), relative energy fluctuations are $\Delta E/E \simeq 10^{-7}$.

All the simulations have been performed using words of 64 bits. We have always chosen random initial conditions at equipartition among momenta.

The convergence of the time averages of Ricci curvature, computed for the FPU model, is fast, so very precise values are easily obtained. We used $N = 128,512$.

For both models, a parallel integration has been made of the dynamics together with Hill's equation (33). The latter has been integrated with the simple central-difference scheme. In these cases Δt has been chosen smaller, $\Delta t = 0.001$, in order to avoid numerical errors in detecting parametric instability.

* Also at INFN, Sezione di Firenze, Largo Enrico Fermi 2, 50125 Firenze, Italy, and INFM, Sezione di Firenze, Largo Enrico Fermi 2, 50125 Firenze, Italy.

[1] M. Pettini and M. Landolfi, Phys. Rev. A **41**, 768 (1990).
[2] M. Pettini and M. Cerruti-Sola, Phys. Rev. A **44**, 975 (1991).
[3] M. Pettini, Phys. Rev. E **47**, 828 (1993).
[4] F. M. Izrailev and B. V. Chirikov, Dokl. Akad. Nauk SSSR **166**, 57 (1966) [Sov. Phys.—Dokl. **11**, 30 (1966)]; B. V. Chirikov, F. M. Izrailev, and V. A. Tayursky, Comput. Phys. Commun. **5**, 11 (1973).
[5] B. Callegari, M. Carotta, C. Ferrario, G. Lo Vecchio, and L. Galgani, Nuovo Cimento B **54**, 463 (1979); G. Benettin G. Lo Vecchio, and A. Tenenbaum, Phys. Rev. A **22**, 1709 (1980); G. Benettin and A. Tenenbaum, *ibid.* **28**, 3020 (1983).
[6] R. Livi, M. Pettini, M. Sparpaglione, S. Ruffo, and A. Vulpiani, Phys. Rev. A **31**, 1039 (1985); R. Livi, M. Pettini, S. Ruffo, and A. Vulpiani, *ibid.* **31**, 2740 (1985).
[7] N. N. Nekhoroshev, Funct. Anal. Appl. **5**, 338 (1971); Russ. Math. Surv. **32**, 1 (1977); G. Benettin, L. Galgani, and A. Giorgilli, Celest. Mech. **37**, 1 (1985); P. Lochak, Phys. Lett. A **143**, 39 (1990).
[8] P. Bocchieri, A. Scotti, B. Bearzi, and A. Loinger, Phys. Rev. A **2**, 2013 (1970).
[9] H. Kantz, Physica D **39**, 322 (1989).
[10] S. Isola, R. Livi, and S. Ruffo, Europhys. Lett. **3**, 407 (1987).
[11] J. Guckenheimer and P. Holmes, *Nonlinear Oscillations, Dynamical Systems and Bifurcations of Vector Fields* (Springer-Verlag, Berlin, 1983).
[12] A. J. Lichtenberg and M. A. Lieberman, *Regular and*

Chaotic Dynamics, 2nd ed. (Springer-Verlag, Berlin, 1992).
[13] L. P. Eisenhart, Ann. Math. **30**, 591 (1929).
[14] G. Benettin, L. Galgani, and J. M. Strelcyn, Phys. Rev. A **14**, 2338 (1976).
[15] E. Fermi, J. Pasta, and S. Ulam, in *Collected Papers of Enrico Fermi*, edited by E. Segré (University of Chicago, Chicago, 1965), Vol. 2, p. 978.
[16] R. Livi, M. Pettini, S. Ruffo, and A. Vulpiani, J. Stat. Phys. **48**, 539 (1987).
[17] *Handbook of Mathematical Functions*, edited by M. Abramowitz and I. A. Stegun (Dover, New York, 1965).
[18] L. Casetti (unpublished).
[19] H. Goldstein, *Classical Mechanics*, 2nd ed. (Addison-Wesley, New York, 1980).
[20] E. Forest and R. D. Ruth, Physica D **43**, 105 (1990).